Spallation Ultracold-Neutron Production in Superfluid Helium

Y. Masuda,[1] T. Kitagaki,[2] K. Hatanaka,[3] M. Higuchi,[4] S. Ishimoto,[1] Y. Kiyanagi,[5] K. Morimoto,[1]
S. Muto,[1] and M. Yoshimura[3]

[1]*High Energy Accelerator Research Organization, 1-1 Oho, Tsukuba, Ibaraki 305-0801, Japan*
[2]*Faculty of Science, Tohoku University, Sendai 980-8578, Japan*
[3]*RCNP, Osaka University, 10-1 Mihogaoka, Ibaraki, Osaka 567-0047, Japan*
[4]*Faculty of Engineering, Tohoku Gakuin University, 1-13-1 Chuo, Tagajo 985-8537, Japan*
[5]*Faculty of Engineering, Hokkaido University, Kita 8 Nishi 5, Kita-ku, Sapporo 060-0808, Japan*
(Received 6 August 2002; published 27 December 2002)

The first ultracold-neutron (UCN) production in superfluid helium placed in a spallation neutron source is carried out. A UCN density of 0.7 UCN/cm^3, which can be used in experiments, is achieved for a proton-beam power of 78 W and a He-II temperature of 1.2 K. The present new UCN source is not limited by Liouville's theorem and extraction losses, which were serious problems in the previous sources. The present source has the possibility of extremely high-density UCN production compared with previous UCN sources.

Ultracold neutrons (UCN), which exist in the low-energy tail of a Maxwellian distribution, have been extracted from cold neutron sources. UCN can be confined in a material bottle and a magnetic bottle. Confined UCN have been used in various experiments, e.g., neutron electric-dipole-moment (EDM) [1] and β-decay [2] experiments. The current interest in the neutron EDM is related to the CP violation and baryon asymmetry in the universe. The weak coupling constants obtained by the neutron β-decay play important roles in the solar neutrino problem, the nucleosynthesis in the universe, and the weak interaction between quarks. UCN are also very useful in other fields, e.g., the quantization under gravity has been observed for the first time with UCN [3].

For further progress in these fields, a high-density UCN source is highly desirable. A turbine UCN converter improved UCN extraction and provided until now the highest UCN density [4]. However, further improvement in the UCN density seems very difficult. UCN density does not change upon deceleration at the turbine according to Liouville's theorem. The turbine does not cool down the neutron temperature, but gets around the transmission loss of UCN through the barrier of the cold neutron source. The UCN density might increase at lower neutron moderator temperature. However, almost all materials are frozen at 20 K, the temperature of cold neutrons. In frozen material, the mass of the scatterer becomes very large, therefore the energy loss of the cold neutron upon scattering is too small to be cooled down further.

UCN production by phonon excitation was proposed [5]. Since Feynman proposed a neutron scattering experiment on superfluid helium (He-II), the Landau dispersion curve and the He-II form factor have been measured by many experiments [6]. The energy-momentum dispersion curves of He-II phonons and neutrons cross in the cold

neutron region. Since phonons behave like neutrons upon collision at the intersection point, energy and momentum are efficiently transferred from neutrons to phonons. Neutrons at the intersection point are cooled down, since the decrease of neutron phase space is balanced with the increase in phonon phase space. The enhancement of UCN production at the intersection point was observed in cold-neutron-beam experiments [7,8]. When He-II is placed in a high flux reactor, an enormous UCN density is obtained. However, γ heating limits the operation of a He-II cryostat in the reactor. The temperature of He-II should be kept below $\sim$1 K in order to suppress up scattering, which is scattering from UCN to higher energy neutrons than the critical energy.

In the present experiment, we produced for the first time UCN in He-II placed in a spallation neutron source where the γ heating is much smaller than in a reactor. UCN were directly transferred to a bottle for experiments and measured. The present method is not limited by Liouville's theorem and extraction losses, therefore realizing a new-generation UCN source.

Solid deuterium (SD$_2$) is also used for UCN production. SD$_2$ has a high UCN production rate, but it has a large loss rate. UCN sources with shutters are being developed to reduce the UCN contact time with SD$_2$ [9–11]. He-II has the advantages of a small loss rate and fast heat conduction, in addition to the lack of extraction losses. These advantages make UCN source operation more effective. The UCN density for long proton pulse is obtained by a product of the production rate and the storage time which is a time constant for UCN loss. We can apply a high proton-beam power to obtain a high UCN production rate. A long storage time in He-II is more effective in lower energies, where a reflection loss rate is lower. Low-energy UCN are crucial for experiments with confined UCN.

Spallation UCN source.—The layout of the present UCN source is shown in Fig. 1. An important advantage of a spallation, compared to a reactor-based neutron source is the small ratio of γ to neutron fluxes. In addition we have the possibility of using a γ-ray shield. A He-II bottle is placed near a lead spallation target, where the neutron flux is very high. A medium-energy proton beam impinges on the 5 cm diam and 20 cm long lead target. Neutrons of energies of several MeV are produced by spallation and are cooled down to thermal energies in an 81 cm diam and 60 cm high heavy water moderator at room temperature. These thermal neutrons are further cooled in a cold moderator of 58 cm diam and 54 cm high heavy water, which is cooled by a Gifford-McMahon cryostat to a temperature of 10 K. A 16 cm diam and 60 cm long He-II bottle is placed inside the cold moderator. The distance from the bottom of the He-II bottle to the spallation target is 28 cm. The bottle is coated with nickel by a nonelectroplating method. The mean potential of the slow-neutron nucleus interaction in matter, which we simply refer to as Fermi potential, is 218 neV for the nickel coating with a small content of phosphorus.

Cold neutrons are down scattered to UCN in the He-II bottle and then UCN diffuse upward. Thin ^{4}He gas at saturated vapor pressure fills the upper part of the He-II bottle. The UCN enter this gas and diffuse to a UCN detector box through an 8.5 cm diam guide tube, which is directly coupled to the He-II bottle without any cryogenic window. The change in the Fermi potential is negligible at the surface of He-II, since the Fermi potential of liquid helium is very small. In the guide tube, ^{4}He atoms collide with the UCN which are almost at rest, but the atomic
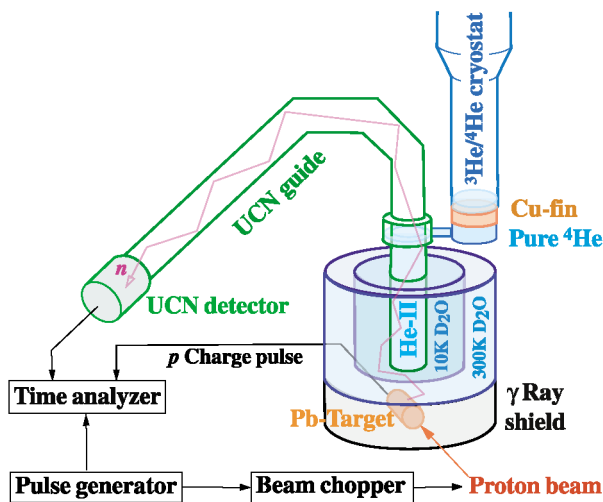

FIG. 1 (color online).   Spallation UCN source. Neutrons are produced by a proton beam in a lead target and then moderated in a cold neutron region in 300-K and 10-K heavy water bottles. These cold neutrons are down scattered to UCN in a He-II bottle. These UCN diffuse via an UCN guide to a detector, where they are measured.

collision rate is small compared with the phonon up-scattering rate. Superfluid film flow does not cause the up scattering because a helium atomic flux originating from the film flow is very small compared with the atomic flux of the gas [12]. The total length of the guide tube from the He-II bottle to the UCN detector box is 2.4 m. The maximum height of the guide tube is 1.2 m above the bottom of the He-II bottle. The gravitational potential for neutrons is 122 neV for the height difference of 1.2 m. For future UCN experiments, an experimental chamber is installed at the end of the guide tube.

The temperature is a key parameter in the new UCN source. The heat load in the He-II estimated by the Monte Carlo simulation code [13] was 7.5 W for a proton beam of 30 kW. The dominant heat load results from the He-II bottle, which is made from 3 mm thick aluminum. The γ heating in the nickel coating is negligible. The He-II is in contact with a copper-fin heat exchanger in a ^{3}He cryostat through four 1 mm diam holes. The He-II is cooled by ^{3}He pumping through the heat exchanger [14]. The temperature gradient in the He-II is negligible. The He-II is one of the best heat conductors. The heat load of 7.5 W in the He-II at 0.8 K can be removed by a ^{3}He pumping of 5000 m^{3}/h. In the present experiment, we used ^{4}He pumping for He-II cooling as the first step. The He-II temperature was 1.2 K at a ^{4}He pumping of 600 m^{3}/h. A temperature rise of about 0.05 K was observed for a heater power of 200 mW.

In the UCN detector box, 1.5 and 2.4 cm diam holes are used as neutron entrance windows. UCN are measured in the following way [15]. ^{6}LiOH-coated films are placed at the windows. The thickness of the ^{6}LiOH coating is 0.5 mg/cm^{2}. No barrier for UCN is placed in front of ^{6}LiOH. Incident neutrons on the entrance windows are captured by ^{6}Li nuclei and then converted to tritons and alpha particles. Half of the charged particles go to Si-PIN diodes. The thickness of the PIN-diode depletion layer is 200 μm, which is longer than the range of the charged particles. A measured pulse height spectrum is shown in Fig. 2. We observed a clear peak in the spectrum resulting from the 2.74 MeV tritons of the ^{6}Li$(n, \alpha)t$ reaction. The small peak of 2.05 MeV α particles is seen in the middle of the spectrum. The steep rise at low energies resulted from γ rays and electric noise. The threshold level was set so that only tritons were counted. The detector efficiency ϵ, given by the ratio of triton counts to the number of neutrons incident on the entrance window, was estimated based on an experiment at the UCN test port of the Institut Laue-Langevin. The efficiency depends on the geometry of the detector. The geometry effect was calculated by a Monte Carlo code. The present detector efficiencies for the small and large detectors were $\epsilon = 3.3\% \pm 0.4\%$ and $6.8\% \pm 0.7\%$, respectively, at a neutron velocity of 5 m/s.

UCN production.—The spallation UCN production in He-II was carried out at the RCNP Ring-Cyclotron
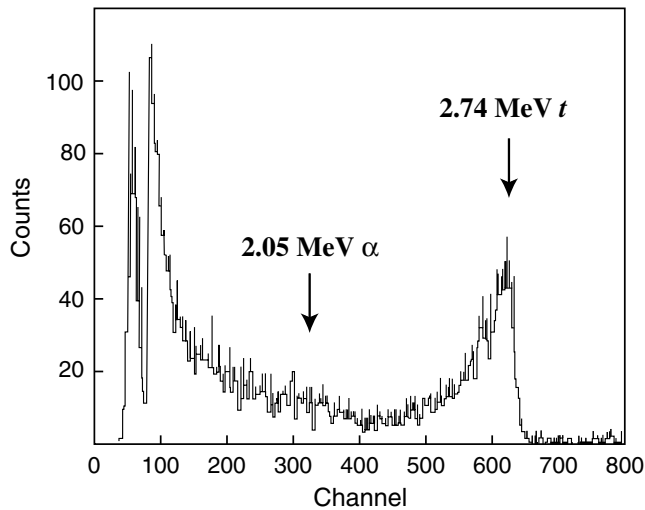
FIG. 2. Pulse height spectrum of UCN detector. The peak labeled 2.74 MeV t results from the tritons of the ^{6}Li$(n, \alpha)t$ reaction. The small plateau (2.05 MeV α) results from alpha particles. γ rays and electric noise produce the steep raise at low energies. The sharp drop below channel 100 results from an overflow.
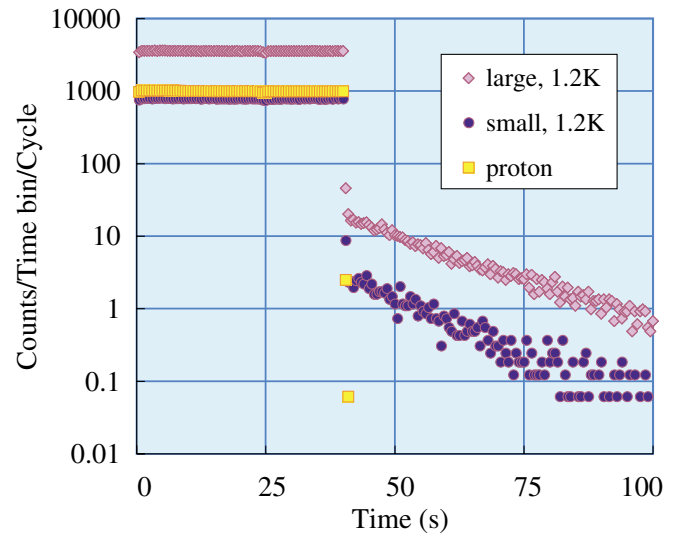

FIG. 3 (color online). Neutron counts as a function of time for a 40 s proton beam pulse. Squares represent proton-charge pulse counts. Diamonds and solid circles show the neutron counts of 2.4 and 1.5 cm diam UCN counters at 1.2 K, respectively. The vertical scale corresponds to counts per time bin for one cycle of proton beam pulse at 200 nA. The time-bin width is 0.5 s.

facility of Osaka University using a proton beam of 392 MeV. The proton beam was pulsed at the injection line of the cyclotron. The peak current of the proton pulse was 200 nA on target. The beam was stopped in the target which worked as a Faraday cup. The charge from the target was accumulated in a current integrator and transformed to a charge pulse every 10^{-10} C. Proton-charge pulses and neutron pulses were counted as a function of time in a VME module.

The neutron decay spectra are shown in Figs. 3 and 4. The squares in Fig. 3 are the counts of the proton-charge pulses. The diamonds and closed circles are the neutron counts of the large and small detectors, respectively. The temperature of the He-II was 1.2 K and did not rise during irradiation by the beam. The neutron counts consisted of two components, prompt and residual counts. After switching the beam off, the prompt counts quickly disappeared. The residual counts resulted from UCN which stayed in a storage bottle consisting of the He-II bottle and the guide tube. A storage time of 14 s was determined from the time constant of the decay spectrum. This value is explained by UCN loss at the detector and the phonon up scattering. We increased the proton-pulse width from 1 to 40 s. The UCN counts increased with the proton-pulse width. The time constant of the increase was consistent with the storage time. In Fig. 3, the pulse width is 40 s. The difference in the neutron counts between the large and small detectors can be explained by the difference in entrance window size and efficiency.

For the confirmation that the residual neutron counts are UCN, we performed measurements with and without nickel foil in front of the detectors. The nickel foil

completely reflects UCN, since the Fermi potential of pure nickel is 252 neV. The thickness of the nickel foil was 8 μm. The window diameters were 1.5 cm. The open and closed circles in Fig. 4 are the neutron counts with and without nickel foil in front of the detectors, respectively. The effect of the total reflection of UCN is clearly shown. The short decay of the neutron counts compared
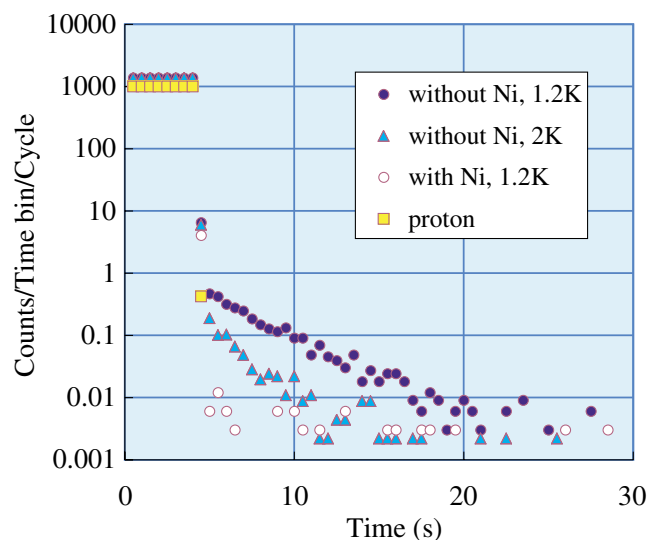

FIG. 4 (color online). Neutron counts as a function of time for a 4 s proton beam pulse. Open and solid circles represent the neutron counts of 1.5 cm diam UCN detectors with and without nickel foil at 1.2 K, respectively. Triangles show the neutron counts of a UCN detector without nickel foil at 2 K.

with Fig. 3 is due to an air contamination in the storage bottle upon detector replacement. We switched off the ^{4}He pumping. When the temperature of the He-II rose to 2 K, the neutron counts decreased faster as shown in the case of triangles. The effect of the phonon up scattering on UCN is clearly shown.

UCN density. — The UCN density at the detector position was estimated by the count rate just after switching off the proton beam. The UCN count rate is represented by the integral $\int 0.25 \rho v A \epsilon dv$, where ρ is a differential neutron density, v the neutron velocity, A the entrance window area, and ϵ the detector efficiency defined above. The UCN density was 0.7 ± 0.1 UCN/cm^3 for the case of a proton beam of 78 W, a UCN storage time of 14 s and a He-II temperature of 1.2 K. The UCN spectrum at production [5] was assumed in the estimation. The error comes from the uncertainty of the detector efficiency.

The UCN density is obtained as a product of the storage time and the production rate which is proportional to the proton-beam power. The UCN density which can be used in an experiment is expected to be 2×10^3 UCN/cm^3 for a 30 kW proton beam and a 100 s storage time. The value is based on the simple extrapolation of the present result. At 0.8 K, the phonon up scattering is negligible [7] so that the UCN storage time becomes 100 s, which is a typical value for a usual storage bottle.

The present setup can be further optimized for higher UCN densities. By surrounding the spallation neutron source with a neutron reflector, the UCN production rate can be increased by a factor of 2 according to the Monte Carlo simulation [13]. If we use beryllium coating for the He-II bottle, the UCN storage density will significantly increase because the confinement potential at the bottom of the storage bottle will increase from 218 to 252 neV, the beryllium Fermi potential. This will also increase the storage time [16]. In addition, if we use a cold deuterium moderator at 20 K, the UCN production rate will also increase. The inelastic scattering probability for low-energy neutrons in liquid deuterium is much higher than in solid heavy water, because deuterons are loosely bound in the liquid. With these improvements, we can expect a significant increase of the UCN density compared to the present setup.

[1] P. Harris *et al.*, Phys. Rev. Lett. **82**, 904 (1999).
[2] P. Huffman *et al.*, Nature (London) **403**, 62 (2000).
[3] V. Nesvizhevsky *et al.*, Nature (London) **415**, 297 (2002).
[4] A. Steyerl, Nucl. Instrum. Methods **125**, 461 (1975).
[5] R. Golub and J. Pendlebury, Phys. Lett. **62A**, 337 (1977).
[6] R. Cowley and A. Woods, Can. J. Phys. **49**, 177 (1971).
[7] R. Golub, C. Jewell, P. Ageron, W. Mampe, B. Heckel, and I. Kilvington, Z. Phys. B **51**, 187 (1983).
[8] H. Yoshiki, K. Sakai, M. Ogura, T. Kawai, Y. Masuda, T. Nakajima, T. Takayama, S. Tanaka, and A. Yamaguchi, Phys. Rev. Lett. **68**, 1323 (1992).
[9] Y. Pokotilovski, Nucl. Instrum. Methods Phys. Res., Sect. A **356**, 412 (1995).
[10] http://lansce.lanl.gov/research/pdf/bowles.pdf
[11] http://ucn.web.psi.ch
[12] G. White, *Experimental Techniques in Low-Temperature Physics* (Clarendon Press, Oxford, 1979).
[13] R. Prael and H. Lichtenstein, Los Alamos National Laboratory, Technical Report No. LA-UR-89-3014, 1989.
[14] Y. Masuda, S. Ishimoto, M. Ishida, Y. Ishikawa, M. Kohgi, and A. Masaike, Nucl. Instrum. Methods Phys. Res., Sect. A **264**, 169 (1988).
[15] T. Kitagaki, O. Konno, M. Higuchi, M. Sato, T. Kawashima, E. Sato, M. Utsuro, and Y. Kawabata, J. Phys. Soc. Jpn., Suppl. A, **65**, 163 (1996).
[16] E. Korobkina and R. Golub (private communication).